Magnetic Conveyor Belt for Transporting and Merging Trapped Atom Clouds

W. Hänsel, J. Reichel, P. Hommelhoff, and T. W. Hänsch
Max-Planck-Institut für Quantenoptik and Sektion Physik der Ludwig-Maximilians-Universität, Schellingstrasse 4, D-80799 München, Germany
(Received 17 August 2000)

We demonstrate an integrated magnetic device which transports cold atoms near a surface with very high positioning accuracy. Time-dependent currents in a lithographic conductor pattern create a moving chain of potential wells; atoms are transported in these wells while remaining confined in all three dimensions. We achieve mean fluxes up to 10^6 s^{-1} with a negligible heating rate. An extension of this device allows merging of atom clouds by unification of two Ioffe-Pritchard potentials. The unification, which we demonstrate experimentally, can be performed without loss of phase space density. This novel, all-magnetic atom manipulation offers exciting perspectives, such as trapped-atom interferometry.

DOI: 10.1103/PhysRevLett.86.608 PACS numbers: 32.80.Pj, 03.67.Lx, 03.75.–b, 39.90.+d

Miniaturization makes it possible to design tightly confining magnetic atom traps with large field gradients and high field curvature without the need for large currents. With lithographic or other surface-patterning processes, microchips can be realized which manipulate (trap, guide, detect, …) neutral atoms in close proximity to the substrate surface. Complex functions may be combined on one chip in order to realize *controllable composite quantum systems* [1], as epitomized by the concept of the quantum computer [2].

We are experimenting with lithographically produced planar conducting patterns in an external magnetic bias field as a means to realize microscopic atom manipulation devices. Although lithographic neutral-atom traps were proposed as early as 1995 [3], the difficulty of loading atoms into such traps has prevented their realization in the past. We have introduced an efficient loading mechanism [4] with the help of a novel mirror-magneto-optical trap (mirror-MOT), using a reflecting layer on top of the circuit pattern to realize the laser fields for laser cooling and trapping in close proximity to the surface. In this way, we were able to demonstrate the first lithographic magnetic trap, a quadrupole trap capturing ^{87}Rb atoms. More recently, the same technique has been applied to construct an Ioffe-Pritchard (IP) trap for ^{7}Li atoms [5]. Integrated parallel conductors have also been used to realize atom guides in which atoms are confined in two dimensions and move freely along the third [6,7]. A different, but related approach was described in [8], where a combination of permanent surface fields and an external bias field produces a series of parallel magnetic tubes, which propagate as the bias field vector rotates. In this experiment, too, the mirror-MOT plays a crucial role in loading the magnetic tubes.

Here we demonstrate a "magnetic conveyor belt," an integrated magnetic device proposed in [4], which transports trapped atoms to very precisely controlled positions near a surface. While the atoms are transported, they remain trapped in all three dimensions, the rms extension of the trap ground state being on the order of 1 μm. This feature distinguishes the conveyor belt from other transport devices such as magnetic guides. It enables the conveyor belt to become a key ingredient in applications with controlled interactions, like quantum computing with trapped atoms, where it can be used to position atoms in an interaction zone for a variable time [9], or as the transport part of a "qubit conveyor belt" [2]. Indeed, the speed of displacement in the conveyor belt can be freely controlled (or reduced to zero) by adjusting the frequency of modulating currents. This implies, moreover, that the device is capable of transporting atoms adiabatically within well-defined quantum states. As we use a thermal atomic cloud in the experiment (temperature in the 30 μK range), the adiabaticity of the transport is evidenced by the heating rate, which becomes unmeasurably low for sufficiently low transport velocity. In this regime, the mean atomic flux is comparable to that achieved in an atom guide [6].

An extension of the conveyor belt allows the merging of atom clouds trapped in two adjacent IP traps. The transfer is complete and, under suitable conditions, occurs without loss of phase space density. We demonstrate this unification process experimentally.

Figure 1 shows the conductor pattern used in the experiment. It is a slightly modified version of the layout proposed in [4]. The width of all relevant conductors is 50 μm. In the simplest case, one can create a quasi-2D IP trap by applying the current I_0 to the center wire and superimposing the bias field $\mathbf{B} = B_{0,x}\mathbf{e}_x + B_{0,y}\mathbf{e}_y$. The trap center forms at distance $r_0 \approx \frac{\mu_0}{2\pi}\frac{I_0}{B_{0,y}}$ from the surface, and if the distance r_0 is much smaller than the length

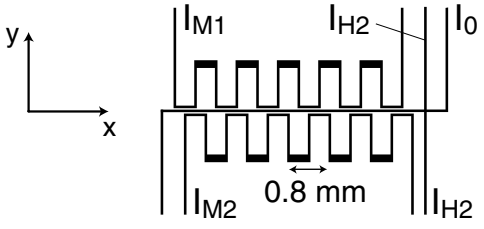

FIG. 1. Layout of the lithographic gold wires on the substrate.

 0031-9007/01/86(4)/608(4)$15.00

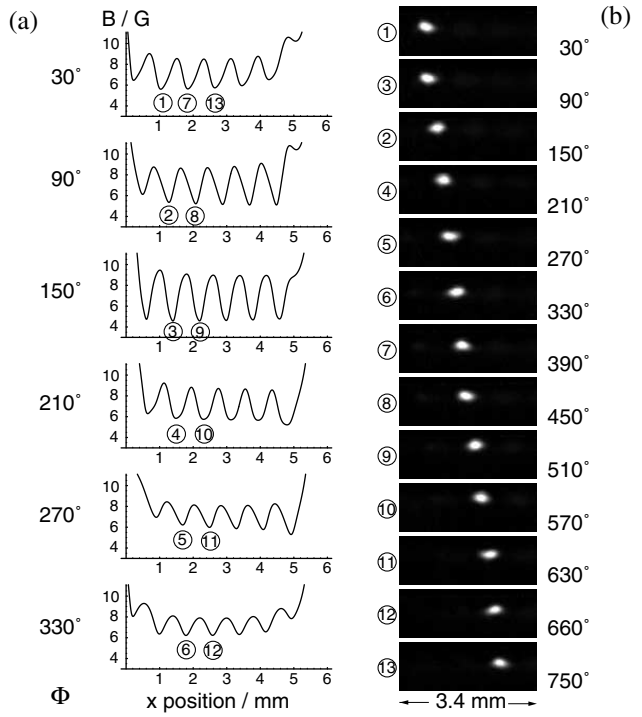

FIG. 2. (a) Conveyor belt potential: For each x position the minimum magnetic field strength in the $\mathbf{e}_y$-$\mathbf{e}_z$ plane is shown. The potential is created by applying the currents $I_0 = 2$ A, $(I_{\mathrm{M1}}, I_{\mathrm{M2}}) = 1\ \mathrm{A}(\cos\Phi, -\sin\Phi)$ in the wire configuration of Fig. 1 and superimposing a constant bias field $\mathbf{B}_0 = 7\ \mathrm{G}\mathbf{e}_x + 16\ \mathrm{G}\mathbf{e}_y$. (b) Absorption images of an atom cloud transported in this potential. In this experiment, $\Phi = 2\pi t/150$ ms, leading to an average transport speed of $\overline{v} = 5.3$ mm/s.

of the center wire (5.5 mm in this setup), the longitudinal potential is boxlike with a minimum field strength of $B_{\mathrm{min}} \approx B_{0,x}$.

The conveyor potential as displayed in Fig. 2(a) is formed starting from such a boxlike potential. The field component $B_{0,x}$, which determines the minimum field strength in the transverse ($\mathbf{e}_y$-$\mathbf{e}_z$) plane, is modulated by means of the currents I_{M1} and I_{M2}. Like a bucket chain, the resulting potential consists of a chain of trapping wells that can be continuously displaced along $\mathbf{e}_x$ by adjusting the currents I_{M1} and I_{M2}. For the potential in Fig. 2(a), a constant current $I_0 = 2$ A and the bias field $\mathbf{B}_0 = 7\ \mathrm{G}\mathbf{e}_x + 16\ \mathrm{G}\mathbf{e}_y$ are applied while the modulation currents

$$(I_{\mathrm{M1}}, I_{\mathrm{M2}}) = 1\ \mathrm{A}(\cos\Phi, -\sin\Phi) \qquad (1)$$

create the local minima. As can be seen from Fig. 2(a), the phase angle Φ determines the x position of the minima, so that they can be displaced continuously over the whole length of the conductor pattern. The depth of the individual wells, i.e., the magnetic field difference between the bottom of a well and the saddle point between two adjacent wells, is 2.5 G on average and varies depending on the phase Φ [cf. Fig. 2(a)]. Transverse ($\mathbf{e}_y\mathbf{e}_z$-plane) curvatures are between 2.5×10^4 G/cm^2 and 4×10^5 G/cm^2 near the bottom of the well, leading to oscillation frequencies between 200 and 800 Hz. Longitudinal frequencies are smaller by a factor of $\sim$4.

The experimental setup is an improved version of the one used in [4] and is described in detail in [10]. Planar gold conductor patterns are formed on an aluminum nitride substrate using a standard microelectronics process known as *thin-film hybrid technology* (a combination of photolithography and electroplating); the wire thickness (height) is 7 μm. We load the microtrap from the mirror-MOT [4] (see also [11]), using a reflecting silver layer on top of the circuit pattern. A thin ($\approx$20 μm) epoxy intermediate layer insulates the circuit pattern from the mirror layer. The MOT is loaded from background vapor (total pressure in the 10^{-10} mbar range). It typically produces 4×10^6 cold atoms within a loading time of 5 s. The atom number is limited by the small diameter and intensity of our trapping beams ($1/e^2$ diameter of 8.5 mm, total power 14 mW). The temperature is 30 μK and the peak density is in the 2×10^{10} cm^{-3} range after a short optical molasses phase. The initial MOT employs a "macroscopic" quadrupole field created by external coils and is loaded $\sim$1 mm away from the surface. The cloud is shifted towards the surface; next, the coils are switched off and a "microscopic MOT" field with the same orientation is created by switching on I_0 and I_{M2} and a bias field along $\mathbf{e}_y$. This combination yields a chain of quadrupolelike potentials. Depending on the position of the shifted MOT, one or several of these small MOTs can be filled with cold atoms. We use both options, depending on the nature of the experiment.

The substrate is mounted upside down in the vacuum cell, so that the atoms are "hanging" below its surface (Fig. 3). Thus, time-of-flight (TOF) images can be taken of the atomic cloud released from the magnetic trap to infer its temperature. We observe the atoms by absorptive imaging, using a probe beam along the $\mathbf{e}_y$ axis. The images show the horizontal $\mathbf{e}_x$ axis (which is the direction of transport) and the vertical $\mathbf{e}_z$ axis. The resolution of the imaging system is 20 μm. Sensitivity is sufficient to detect 30 atoms per pixel without averaging.

The loading procedure ends with an optical pumping pulse which pumps the atoms to the $F = 2, m = 2$ ground state. After this pulse, the magnetic potential is switched on. Here, the initial potential is the conveyor belt

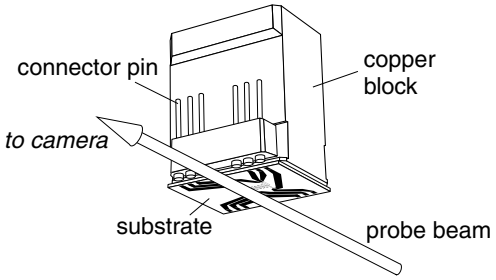

FIG. 3. Experimental geometry.

potential (cf. Fig. 2) with the parameter $\Phi = 0$, i.e., $I_0 = 2$ A, $I_{M1} = 1$ A, and $I_{M2} = 0$. With this phase value, the positions of the well centers coincide with those of the quadrupole fields in the previous microscopic MOT, so that atoms are efficiently transferred. We typically obtain trapped clouds with $1/\sqrt{e}$ radii $\sigma_x \approx 113$ μm and $\sigma_y \approx 71$ μm, which contain $\sim 1.5 \times 10^5$ atoms with a peak density of 1.5×10^{10} cm^{-3}. The $1/e$ lifetime is about 4 s, limited by the background pressure of rubidium and other residual gases.

At this point, the conveyor belt is started by varying the phase Φ. Figure 2(b) shows absorption images of the transport process. (As the imaging is destructive, each image is taken starting from a "fresh" trapped sample.) The center-of-mass position of the atom cloud is extracted from these images and is plotted in Fig. 4 as a function of Φ. In this example, the phase Φ is made to increase linearly with time, $\Phi = \omega t$ with $\omega = 2\pi/150$ ms. It should be emphasized, however, that *any* function of time can be used to control the phase: the atom cloud can be accelerated, or moved at constant speed, or be stopped at any desired position. The positioning accuracy is ultimately limited only by the ground state size, which is 0.9 μm FWHM for the 800 Hz oscillation frequency attained in this potential. The position uncertainty introduced by current fluctuations is orders of magnitude below this value.

In most applications, it is essential to minimize heating of the trapped cloud during the transport. Leaving aside external mechanisms such as heating by the surface (which is negligible at our atom-surface distance of more than 50 μm), transitions may be induced only by the deformation and displacement of the potential wells during the shifting process. The rate of such transitions should decrease to insignificant levels when the speed of displacement is low enough. In our present experiment, where many vibrational states are populated, these transitions translate into heating. We therefore measured the final temperature of the cloud as a function of the maximum shift velocity v_{max} (Fig. 5). For decreasing transport speed, the heating rate decreases, as expected, and becomes unmeasurable within our ± 2 μK accuracy for speeds $v_{max} \leq 0.5$ cm/s. In this sense, the transport is adiabatic. When consecutive potential wells are filled with $\sim 1.5 \times 10^5$ atoms each, the shifting process results in a mean flux of 9.4×10^5 s^{-1}. In a future experiment where single vibrational levels are populated, it will be possible to verify adiabaticity on the quantum mechanical level.

The above data demonstrate the ability to move and position the atom cloud. The conveyor belt can be employed in complex experiments needing precise atom positioning, such as those discussed in the introduction. As another example, it may be used in cavity QED experiments to transport atoms into and out of a zone where they interact with a high-finesse optical resonator, such as a miniature Fabry-Pérot resonator [12,13] or a silica microsphere [14,15]. In this way, long and reproducible interaction times and precise positioning of the atomic sample within the quantized resonator field can be achieved. Such a coupling would also enable nondestructive atom detection, as required for quantum computing. Another, more macroscopic application of the conveyor belt would be to transport cold atoms from a production region into a spatially separated interaction region, providing an integrated version of the coil-based magnetic transport device which was recently realized in our laboratory [16].

One advantage of the lithographic technique is the ability to combine different potentials very easily. With only one additional wire (I_{H2} in Fig. 1), a stationary IP trap can be formed at the end of the conveyor belt, which adds new options of atom cloud manipulation. The depth of the stationary trap is controlled by current I_{H2}, independently of the conveyor belt movement. Figure 6(a) shows the resulting potential when $I_{H2}(\Phi)$ (directed along $-\mathbf{e}_y$) is varied according to $I_{H2} = 0.462 + 0.255 \sin(\Phi + 0.493) - 0.088 \sin(2\Phi - 1.482)$, while all other parameters are controlled as before. (The figure shows only the right part of the potential; cf. Fig. 2.) Once per period the stationary trap above H_2 continuously unites with the conveyor belt trap arriving from the left. The unification takes place by lowering the barrier between the two traps.

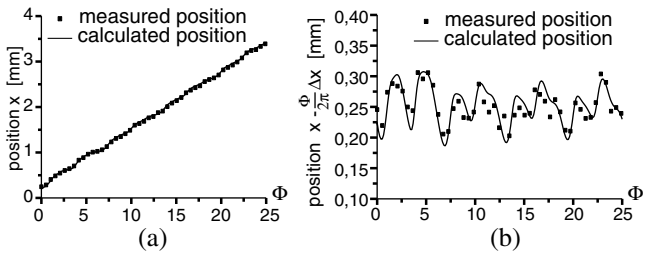

FIG. 4. (a) Position of an atom cloud transported in the potential of Fig. 2(a). The center of mass is shown as a function of the phase angle Φ, which is varied according to $\Phi = \omega t$ with $\omega = \frac{2\pi}{150\ \mathrm{ms}}$. The fact that the x position is not strictly linear in Φ is due to the particular form of the modulation wires and is well reproduced in the simulation as can be seen in (b) where the linear part of $x(\Phi)$ is subtracted.

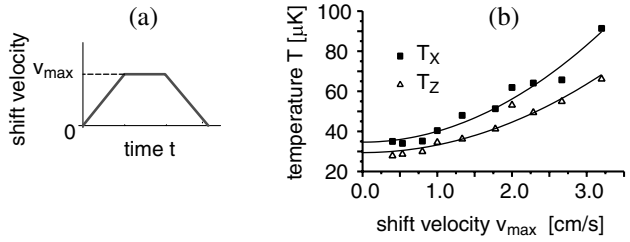

FIG. 5. (a) The shift velocity is increased linearly during one spatial period (0.8 mm), then kept constant for two periods (1.6 mm), and ramped back to zero during the last period. (b) The heating rate decreases for slow transport. The difference between T_x and T_z for slow speeds is due to incomplete thermalization during the preparation stage. For increasing v_{max}, T_x grows more rapidly than T_z, indicating that heating occurs predominantly in the transport direction.

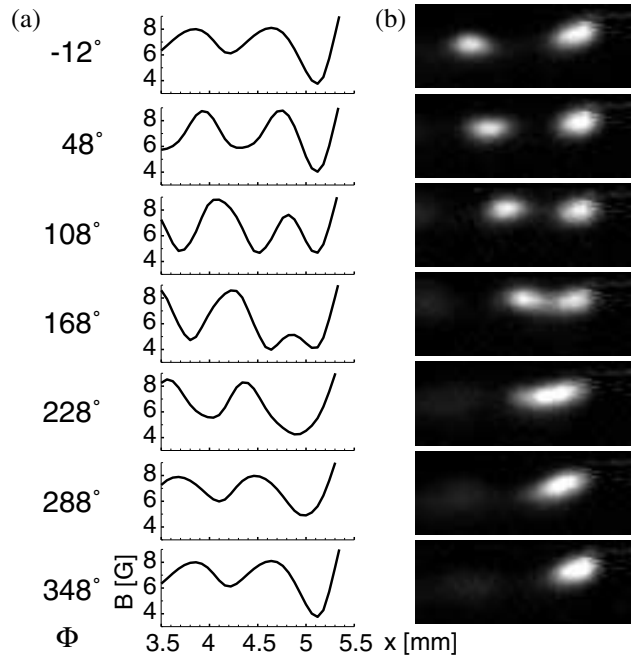

FIG. 6. (a) Right part of the magnetic conveyor belt potential when an additional current I_{H2} is applied (see text). All other currents and fields are as in Fig. 2. During one cycle of Φ, the potential well arriving from the left unites with the stationary, right well, which is then compressed back to its original size while the next well approaches. (b) Unification of two atom clouds in this potential.

At $\Phi \approx 100°$, the two traps are still fully separated. At $\Phi \approx 210°$, their separation has vanished, and at $\Phi \approx 350°$, the united trap has been compressed to the volume originally occupied by the stationary trap. Thus, the process is similar to the classical thermostatistical problem of pulling a septum out of a container, followed by slowly reducing the container's volume (Fig. 7). In particular, if each trap initially contains N atoms at equal temperatures and densities, then after one complete cycle, the cloud in the stationary trap should have the same phase space density as before. As it now contains $2N$ atoms, temperature must have increased during the unification.

We have implemented this process experimentally by loading two conveyor traps from the MOT and then applying the current modulation described above. Figure 6 shows the computed potentials (a) as well as absorption images (b) of different stages of the unification process. The potentials have been designed in a way that equally populated traps should merge without loss of phase space density. Because of the difficulty of performing TOF measurements on the two neighboring clouds, we have not yet been able to measure the phase space density during this process. Instead one can infer the properties of the unification process by the decrease of phase space density when only one of the two potential wells is initially populated.

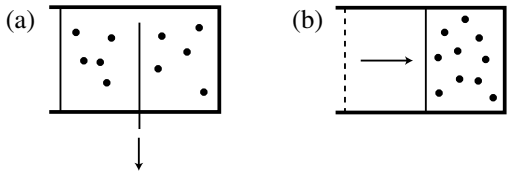

FIG. 7. Simple thermodynamic model idealizing the potential of Fig. 6(a): isolated container divided into halves by a septum. (a) The septum is pulled out. In the special case where each half initially contains N atoms at temperature T_0, the temperature, density, and also the phase space density remain unchanged. (b) The volume is adiabatically reduced by a factor of 2 by slowly moving one of the walls. Again, the phase space density remains constant. Thus, the complete process doubles the number of atoms in the right volume without changing the phase space density.

For this situation, we measure a decrease of ≈ 0.6 per unification, which is close to the decrease of 0.5 expected for the unification of two identical traps one of which is empty.

The unification sequence can also be reversed. In this case, an atom cloud initially localized in the stationary trap is separated into n parts during n periods. If the separation is done slowly, the process is adiabatic, opening intriguing possibilities for the manipulation of atomic wave packets, including interferometers with trapped atoms. A quantitative study of the unification and separation processes is currently under way.

This work is supported in part by a grant from the European Union (ACQUIRE project, Contract No. IST-1999-11055).

[1] P. Zoller, Nature (London) **404**, 340 (2000).
[2] See, for example, D. P. DiVincenzo, quant-ph/0002077.
[3] J. D. Weinstein and K. G. Libbrecht, Phys. Rev. A **52**, 4004 (1995).
[4] J. Reichel, W. Hänsel, and T. W. Hänsch, Phys. Rev. Lett. **83**, 3398 (1999).
[5] R. Folman *et al.,* Phys. Rev. Lett. **84**, 4749 (2000).
[6] D. Müller *et al.,* Phys. Rev. Lett. **83**, 5194 (1999).
[7] N. H. Dekker *et al.,* Phys. Rev. Lett. **84**, 1124 (2000).
[8] P. Rosenbusch *et al.,* Phys. Rev. A **61**, 031404(R) (2000).
[9] T. Calarco *et al.,* Phys. Rev. A **61**, 022304 (2000).
[10] J. Reichel, W. Hänsel, P. Hommelhoff, and T. W. Hänsch (to be published).
[11] T. Pfau and J. Mlynek, OSA Trends Opt. Photonics Ser. **7**, 33 (1997).
[12] C. J. Hood *et al.,* Science **287**, 1447 (2000).
[13] P. W. H. Pinkse, T. Fischer, P. Maunz, and G. Rempe, Nature (London) **404**, 365 (2000).
[14] F. Treussart *et al.,* Opt. Lett. **19**, 1651 (1994).
[15] D. W. Vernooy *et al.,* Phys. Rev. A **57**, R2293 (1998).
[16] M. Greiner, I. Bloch, T. W. Hänsch, and T. Esslinger (to be published).